Available online at www.sciencedirect.com

SCIENCE DIRECT®

Applied Surface Science 234 (2004) 333–340

applied surface science

www.elsevier.com/locate/apsusc

# Relation between morphology and work function of metals deposited on organic substrates

T.U. Kampen[a,*], A. Das[b], S. Park[c], W. Hoyer[a], D.R.T. Zahn[a]

[a]*Institut fur Physik, TU Chemnitz, D-09107 Chemnitz, Germany*
[b]*Physics Department, University of Wales, Cardiff, Wales, UK*
[c]*Paul Scherrer Institute, CH-5232 Villigen, Switzerland*

## Abstract

Ultraviolet photoemission spectroscopy (UPS) is employed to determine the work function of silver and indium films grown on two perylene derivatives, dimethylen-3, 4, 9, 10-perylenetetracarboxyiimide (DiMe-PTCDI) and 3, 4, 9, 10-perylenetetracarboxylic dianhydride (PTCDA). The PTCDA and DiMe-PTCDI substrates were prepared as thick organic layers on sulphur passivated GaAs(0 0 1), where the molecular planes of PTCDA and DiMe-PTCDI are parallel and tilted with respect to the substrate surface, respectively. The crystalline structure of the evaporated metal layers is investigated using X-ray diffraction (XRD) and is found to be strongly dependent on the underlying organic substrate. Correspondingly, work functions are found to be different by more than 200 meV in agreement with the crystalline orientation of the metal films.

*Keywords:* Ultraviolet photoemission spectroscopy; X-ray diffraction; DiMe-PTCDI

## 1. Introduction

In organic electronics, metals evaporated onto organic molecular films play an important role as electrodes for charge injection. While low work function materials are used for electron injection, metals with a large work function are used for hole injection. In many cases, the carrier injecting electrodes are prepared by evaporating metals on organic layer. It should be noted that these metal-on-organic interfaces are different from organic-on-metal interfaces in that metallisation chemistry and interdifusion can occur [1–3].

Quite often the vacuum level alignment is used to determine the energy level alignment at metal/organic interfaces, which is the analogue of the Schottky–Mott limit for inorganic semiconductors. Here, it is assumed that the vacuum levels of the materials in contact align at the interface. The interface barrier heights can be determined by simply calculating the difference between the metal work function and the ionisation potential and electron affinity for a semiconductor doped p- and n-type, respectively. Detailed studies have demonstrated that metal/organic interfaces are more complex than originally anticipated. For example, a conclusion that in general the vacuum levels do not align has been reached [4–7]. The difference in vacuum levels is attributed to a charge transfer across

---

[*] Corresponding author. Present address: Abteilung Molekülphysik, Fritz-Haber-Institut der Max-Planck-Gesellschaft, Faradayweg 4-6, 14-195 Berlin, Germany. Tel.: +49-30-8413 5654; fax: +49-30-8413 5603.
*E-mail address:* Kampen@fhi-berlin.mpg.de (T.U. Kampen).

0169-4332/$ – see front matter © 2004 Elsevier B.V. All rights reserved.
doi:10.1016/j.apsusc.2004.05.061

the interface resulting in interface dipoles. Interface dipoles as large as 1.5 eV have been found which significantly affect the magnitude of charge injection barriers [5,8–11]. An important aspect for metal-on-organic interfaces is the work function of the evaporated metal, which strongly depends on the crystalline structure and morphology of the film. This issue of how the morphology of metal electrodes and their work function is correlated with the molecular and crystalline structure of the underlying organic substrate has not been investigated in detail and is the topic of this contribution.

Despite the above mentioned charge transfer across the interface, other mechanisms like polarised chemical bond formation or the electronic image force outside a metal surface [10] have been discussed as possible sources for interface dipoles. Peisert et al. investigated interfaces between Au and different phthalocyanine molecules and found two contributions to the potential drop across the interface [12]. The larger one of these contributions results from an alignment of the Fermi levels at the interface resulting in a strong potential drop within the first 2 nm from the interface, which is linearly dependent on IP $-1/2E_t$ with a slope of one. Here, IP and $E_t$ are the ionisation potential and the transport gap [13] of the organic materials. The second much smaller contribution is a potential drop in the organic extending up to 10 nm from the interface into the organic film.

Such ‘‘band bending’’-like electrostatic energy shift in organic layers has been observed in many metal/organic systems [14]. In most cases this shift is confined to a regime of only a few nanometers, which cannot be accounted for using the conventional band bending theory of inorganic semiconductors. Shifts occurring in such small thickness ranges can be due to a change in the intermolecular interaction, namely, due to a change in the molecular orientation as a function of the film thickness, or due to a change in polarisation energy induced by the interaction with metal atoms. The change in the molecular orientation thus produces a band bending or energy level shift that plays an important role in the actual device properties. This observation has been made for copper phthalocyanine (CuPc) films grown on $MoS_2$ substrates.

Another physical mechanism resulting in shifts of the Fermi level are gap states, which are the most relevant mechanism at inorganic semiconductor interfaces. For organic materials the existence of interface gap states is currently under investigation. They have been observed in long-chain alkane films [15] and at interfaces of Mg, Ca or Li on $Alq_3$, [16–18] and Ag on 3, 4, 9, 10-perylenetetracarboxylic bisimidazole (PTCBI) [19]. These states are often referreed to as polaron or bipolaron states. Polarons are singly occupied and represent a half-filled orbital, which should occur at the Fermi level. Since organic molecules represent small systems with localised charge electrons, the Coulomb repulsion between the first and second electrons placed in this orbital results in the opening of a Coulomb gap, such that the singly-occupied polaron state will occur below the Fermi level. Bipolaron states are doubly occupied [20].

Hirose et al. investigated the chemical and electronic properties of interfaces between PTCDA films (40–80 nm) and In, Al, Ti, Sn, Au and Ag using synchrotron radiation photoemission spectroscopy [21]. In, Al, Ti and Sn are found to react at room temperature with the oxygen containing anhydride group of the PTCDA molecule. The result of these reactions are interface states in the band gap of PTCDA. The penetration of the reactive metals is found to be inversely related to their first ionisation energy whereby ionised metals are driven into the PTCDA film by Coulomb repulsion. For In, the penetration depth is found to be above 10 nm. All reactive metals result in ohmic contacts which is attributed to carrier conduction through interface gap states. For the noble metals Au and Ag no interface reaction and diffusion is observed which results in a blocking concerning carrier transport. The In/PTCDA system was investigated in more detail by Azuma et al. [22]. Here, only a monolayer of PTCDA was prepared on cleaved $MoS_2$. They also observed In-induced interface states in the band gap of PTCDA. These states are attributed to the reaction between In and PTCDA resulting in a $In_4$PTCDA compound. A comparison of molecular orbital calculations and angular resolved photoemission measurements shows that the gap states can be explained by the calculated density of states of the $In_4$PTCDA complex, where the gap states originate from the π-orbital which consists of carbon $2p_z$, oxygen $2p_z$, and indium $5p_z$ atomic orbitals. Cs deposition on PTCDA is also known to produce gap states, observed in the VB spectra by Ertl et al. [23]. However, their MO calculation shows that even without a covalent bond between

Cs and PTCDA, the charge transfer can occur through O atoms in the anhydride and the carboxylic group. As such, it is still under debate whether and where in the molecules a chemical reaction occurs at metal/PTCDA interfaces.

Here, indium and silver were evaporated on PTCDA and DiMe-PTCDI films prepared on sulphur passivated GaAs(1 0 0) surfaces. The orientation of molecules in PTCDA films is found to be parallel substrate surface, which is equivalent with the (1 0 2) crystalline plane being parallel to the (1 0 0) plane of GaAs. For DiMe-PTCDI the angle between the (1 0 2) plane of crystalline domains is tilted with respect to the substrate plane by approximately 58° [24].

## 2. Experimental

Tellurium doped *n*-GaAs(1 0 0) with a doping concentration of $N_D = 2 \times 10^{17}\,\mathrm{cm}^{-3}$ (Freiberger Compound Materials) served as substrate for the organic thin films. The substrates were passivated with sulphur since a chalcogen passivation of GaAs(1 0 0) surface was found to improve the crystalline quality of organic films [25,26]. Sulphur passivation was obtained by a wet chemical etching procedure under atmospheric conditions [27]. This etching procedure consists of a sequence of three steps. After cleaning in degreasing solvents, the GaAs was dipped into a solution consisting of a 3:1 mixture of $CCl_4$ and $S_2Cl_2$ for 10 s. In the last step the substrate was rinsed successively in $CCl_4$, acetone, ethanol and deionised water for 5 s each. After this treatment the substrate was transferred into a UHV system and annealed at 430 °C. This procedure leads to a well ordered, (2 × 1) reconstructed surface as revealed by low energy electron diffraction (LEED) [28].

The sample preparation and the characterisation using ultraviolet photoemission spectroscopy (UPS) were performed in two interconnected UHV systems having base pressures of about $3 \times 10^{-8}$ Pa. PTCDA (Lancaster) or DiMe-PTCDI (Syntec GmbH) were purified by vacuum sublimation. The organic materials were deposited under ultra high vacuum conditions onto the modified GaAs surfaces with the thickness controlled by a quartz microbalance located in the vicinity of the sample. Deposition rates were between 0.3 and 0.8 nm/min. For comparison, the distance between the molecular planes in a PTCDA crystal corresponds to 0.32 nm [29]. Silver and indium were evaporated with a deposition rate of 7 nm/min.

Valence band spectra were recorded with an angle resolved UPS system (VG ARUPS 10), and a He discharge lamp ($h\nu = 21.22$ eV). The overall resolution measured from the Fermi edge of polycrystalline Ag(1 1 1) is 0.15 eV. A sample bias of−9 V was applied to the sample to determine the sample work function. The ionisation energy of the organic film and its changes upon metal deposition was determined by taking the difference between the vacuum level position, measured using the secondary electron onset of the photoemission spectrum, and the top of the highest occupied molecular orbital (HOMO) defined as the intercept between the tangent to the low binding energy side of the HOMO and the background level.

X-ray diffraction and X-ray reflectivity measurements were made using a SEIFERT 3000 PTS diffractometer with Cu Kα ($\lambda = 1.5415$ Å) radiation. The X-ray generator is operated at 40 kV and 20 mA. A bending graphite monochromator is placed at the detector side. Soller slits were also included at both sides of the incident and reflected beams to limit any axial divergence. For recording the diffraction spectrum, $\theta$–$2\theta$ scans in the range of 5°–80° with a step width of 0.02° were carried out in Bragg–Brentano geometry.

## 3. Results and discussion

### *3.1. Ag/PTCDA and Ag/DiMe-PTCDI*

Fig. 1 shows valence band spectra of clean PTCDA and DiMe-PTCDI and after successive Ag depositions. At Ag coverages below ~1 nm, all features from the PTCDA and DiMe-PTCDI films can still be seen. The line shapes and energy positions of these features are not changed, indicating that the chemical interaction between Ag and the organic materials is very low and that there is no Ag-induced band bending in PTCDA and DiMe-PTCDI. This is in agreement with the results by Hirose et al. who found that the lineshape of the Cls core level emission of PTCDA is not changed upon deposition of 4 nm of Ag [1]. In addition, two small Ag-induced features appear in the HOMO–LUMO gap of the organic films (R1’,R2’ and

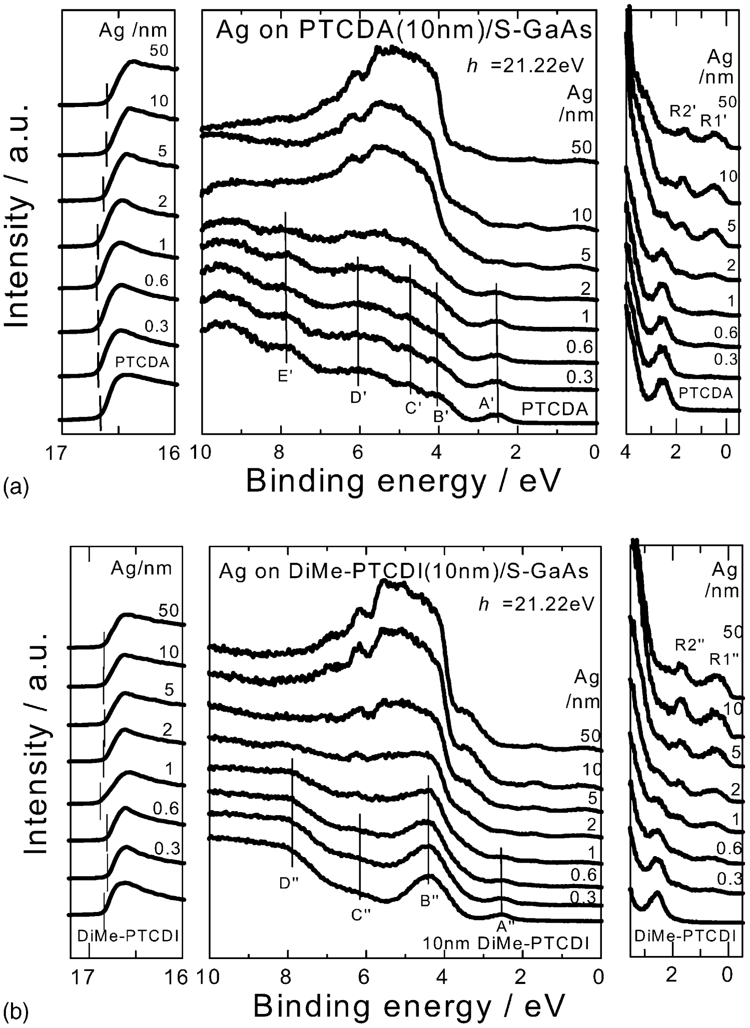

Fig. 1. VB spectra as a function of Ag thickness on (a) 10 nm PTCDA and (b) 10 nm DiMe-PTCDI films. (*hν*= 21.22 eV). Solid lines are guides for the eye.

R1”,R2”). The energy positions of those features are at 0.5 eV and 1.7 eV below the Fermi edge. It should be mentioned that such bands have also been observed for the growth of PTCDA on Ag single crystal surfaces and are attributed to the organic film [30]. The Fermi edge becomes visible above 2 nm. This thickness is four times larger than the thickness, for which a Fermi edge is observed for Ag films grown on chalcogen passivated GaAs(1 0 0) surfaces (0.5 nm). This can be attributed to a diffusion of Ag into the organic layers, which will reduce the actual thickness of Ag on the surface, and a stronger clustering of Ag on the DiMe-PTCDI. Therefore, a metallic behaviour will be observed at higher nominal coverages. On the other hand, the UP spectra in Fig. 1 show that there is no interaction between the Ag and the organic materials. Therefore, diffusion of Ag takes place only via the grain boundaries between adjacent crystallites, but not into the crystallites. This is also confirmed by Raman investigations [31]. These Raman investigations also show the formation of dynamic charge transfer complexes.

The Rl, and R2, (Rl” and R2”) bands can still be observed for a fairly high coverage with a maximum in intensity for a nominal coverage of 10 nm. As mentioned above, there is a substantial diffusion of the Ag into the PTCDA film which reduces the actual surface coverage of the organic film. On the other hand, the Ag films grown on PTCDA and DiMe-PTCDI are polycrystalline, as will be shown in the next section. These findings, and the fact, that the density of states of Ag is very low in the binding energy range where the Rl, and R2, (Rl" and R2") bands are located, leads to the low attenuation of the features as a function of the nominal coverage. The evolution of the work function as a function of the thickness of Ag is shown in Fig. 2a. The values for single crystal Ag(1 1 1) and polycrystalline Ag films are included [32,33]. Before Ag deposition, the $\phi$ values of PTCDA and DiMe-PTCDI are (4.56 ± 0.05) and (4.38 ± 0.05) eV, respectively. Upon deposition of Ag on PTCDA, a slight decrease of $\phi$ is observed up to 1 nm and then $\phi$ begins to increase gradually to reach a final value of (4.61 ± 0.05) eV. On the other hand, $\phi$ does not change over all Ag deposition upon DiMe-PTCDI.

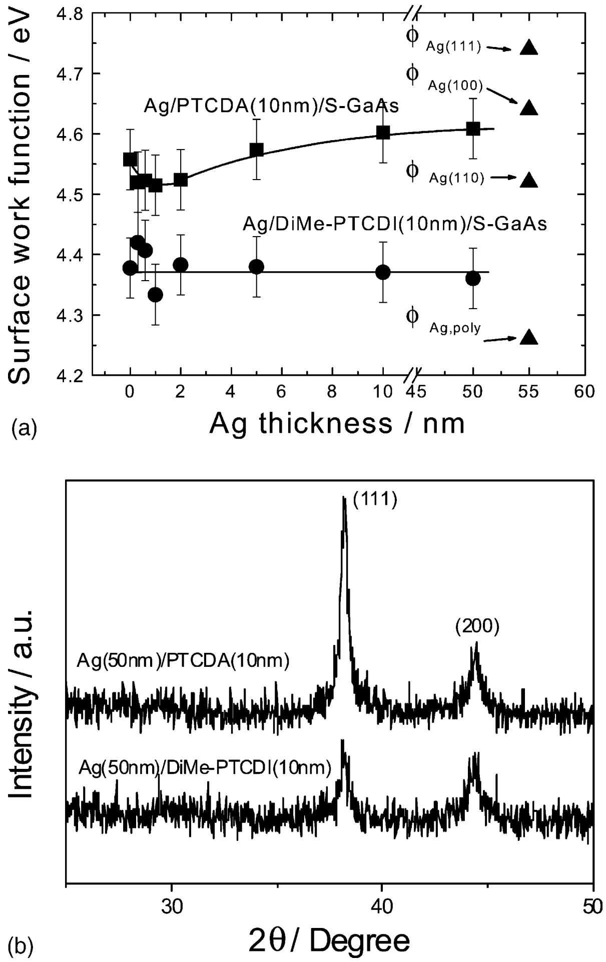

Fig. 2. (a) The evolution of $\phi$ as a function of Ag thickness deposited on 10 nm films of PTCDA and DiMe-PTCDI. For comparison values of $\phi$ for the polycrvstalline Ag film and single crystalline Ag(1 1 1) are included. Solid lines are guides for the eye. (b) XRD spectra of 50 nm Ag films on the 10 nm PTCDA and DiMe-PTCDI films.

Additional X-ray diffraction (XRD) experiments on the samples reveal two peaks corresponding to the (1 1 1) and (2 0 0) directions with the relative intensity ratios of the two peaks being different depending on the organic substrates (see Fig. 2b). The (1 1 1) peak is much stronger for Ag/PTCDA than Ag/DiMe-PTCDI while the (2 0 0) peak intensities are similar in both cases. Therefore the crystalline structure of the Ag films is strongly affected by the morphology of the underlying organic film.

The difference in $\phi$ for thick Ag films on PTCDA and DiMe-PTCDI can be understood by comparison with the $\phi$ values of Ag with different crystalline structures. The $\phi$ value of the Ag film on PTCDA is closer to the value corresponding to Ag(1 1 1) single crystal. This agrees very well with the observation of a stronger (1 1 1) peak in the XRD experiment. Another interesting point to mention is a transient behaviour of $\phi$ at low Ag coverages. Since at low metal coverage it is expected that metal atoms diffuse into the underlying organic film, $\phi$ reveals the influence of the metal atoms on the organic films. The metal atoms can influence electronic properties of the organic films in two ways. First, in the presence of any charge transfer, whether or not accompanied by the formation of covalent bonds, the energy levels of the organic film close to the surface will change according to the amount of charge transferred from or to the molecules. Second, even if there is no charge transfer, metal atoms between organic molecules in the film can disturb the crystalline structure of the organic layer and, consequently, change the polarisation energy which is defined as the energy difference of *IE* (*EA*) between the isolated molecules and the film. This effect can also lead to a change in the energy levels. In the case of Ag atoms in PTCDA and DiMe-PTCDI, where there is no charge transfer between Ag atoms and the organic molecules, only the change in polarisation energies can affect $\phi$. Hence, the slight decrease in $\phi$ at low Ag coverage on PTCDA can be explained by a disturbance of the organic crystalline structure, followed by the change in polarisation energy.

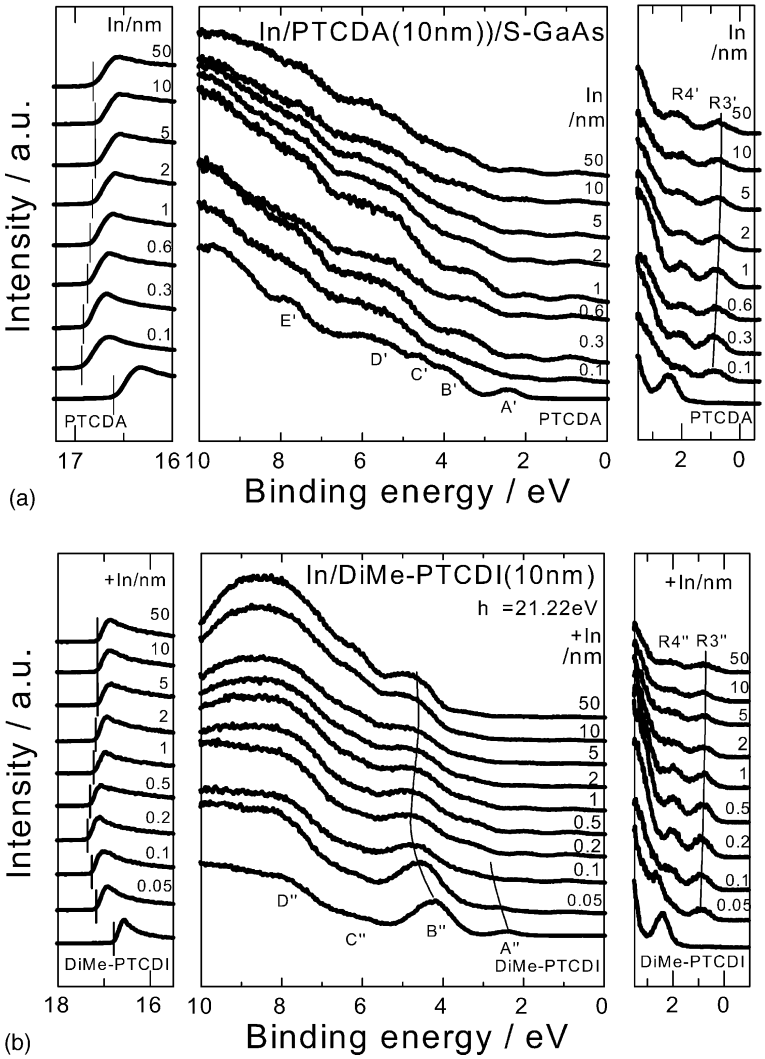

Fig. 3. VB spectra as a function of In thickness on (a) 10 ran PTCDA and (b) 10 ran DiMe-PTCDI films, ($h\nu = 21.22$ eV). Solid lines are guides for the eye.

### 3.2. In/PTCDA and In/DiMe-PTCDI

Fig. 3 shows valence band spectra during deposition of In on 20 nm films of PTCDA and DiMe-PTCDI are shown. Unlike Ag, the deposition of the smallest amount of In (0.1 nm for PTCDA and 0.05 nm for DiMe-PTCDI) changes the spectra significantly, namely, the appearance of two new features (R3',R4' and R3'', R4'') in the HOMO-LUMO gap of the organic films and strong energy shifts are observed in the low kinetic energy onset as well as bands A'' and B'' of DiMe-PTCDI. It is difficult to determine the energy shifts of bands corresponding to the PTCDA film because even at 0.1 nm In thickness they are not visible any more. However, for In/DiMe-PTCDI, the shifts of A'' and B'' towards higher binding energy are unambiguous and the band B'' is visible up to 50 nm In thickness. The new features in the gap are different from those which appear upon Ag deposition (R1',R2', and R1'',R2'' in Fig. 2) in that they are pronounced even at low In thickness. Again, those features can be attributed to the gap states induced by the deposition of metals on organic surfaces, as was also observed by Hirose et al. for metals of In, Sn, Al, and Ti on PTCDA [34]. A large number of In atoms diffuse into the organic films lead to the

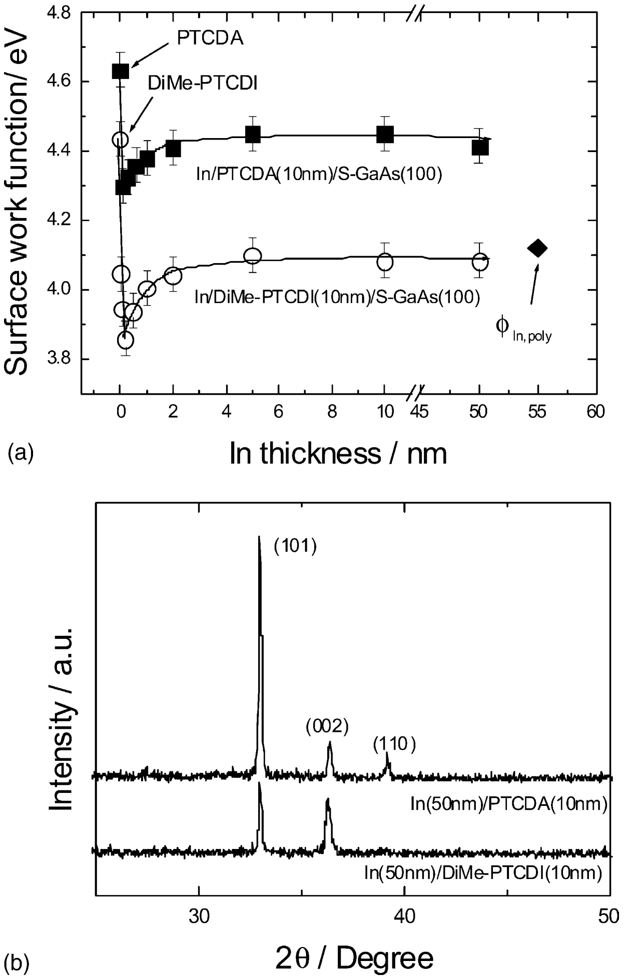

Fig. 4. (a) The evolution of $\phi$ as a function of In thickness deposited on 10 nm films of PTCDA and DiMe-PTCDI. For comparison the value of $\phi$ for the polycrystalline In film is included. Solid lines are guides for the eye. (b) XRD spectra of 50 nm In films on the 10 nm PTCDA and DiMe-PTCDI films.

formation of charge transfer complexes and give rise to large densities of gap states easily detectable via PES [35]. The evolution of $\phi$ is shown in Fig. 4a as a function of In thickness on 10 nm films of PTCDA and DiMe-PTCDI. A very steep decrease in $\phi$ at low In thickness was observed for both molecules, followed by a gradual increase up to final values. As in the case of Ag, the different final values of $\phi$ can be attributed to different crystalline structure and crystallinity of the In layers. The differences between $\phi$ of the bare organic films and the minimum $\phi$ at low In thickness are (0.40 $\pm$ 0.10) and (0.55 $\pm$ 0.10) eV for In/PTCDA and In/DiMe-PTCDI, respectively. This is the reversed situation to Ag deposition on PTCDA and DiMe-PTCDI. In case of In, a charge transfer between In atoms and organic molecules is apparent and the charge transfer contributes to most of the change in $\phi$ , rather than due to the change in the polarisation energy. The $\phi$ change also implies the amount of charge transferred to or from the organic molecules. Our result tells that there is more charge transfer between In and DiMe-PTCDI than between In and PTCDA. This and a substantial diffusion of In into the organic substrates have been found by Raman investigations [36]. Raman spectra also reveal that the inorganic complex formed is a dynamical charge transfer complex. The formation of an $In_4$-PTCDA including the formation of covalent bonds proposed by Kera et al. [37] is not observed. The XRD measurements for the 50 nm In film on PTCDA and DiMe-PTCDI ( Fig. 4b) also show different morphology. For the In film on PTCDA three peaks corresponding to the (1 0 1), (0 0 2), (1 1 0) crystallographic directions are revealed, while the only (1 0 1) and (0 0 2) peaks are visible for In on DiMe-PTCDI. The intensity of the (1 0 1) peak is found to be much stronger for In/PTCDA. Considering also the stronger (1 1 1) diffraction peak for Ag/PTCDA than that for Ag/DiMe-PTCDI, it can be concluded that metal films on PTCDA have higher crystallinity than on DiMe-PTCDI.

## 4. Conclusions

The work functions of Ag and In films vary as a function of the of the organic substrate used for deposition. The different work functions are attributed to the crystalline structure of the evaporated metal layers being strongly dependent on the underlying organic substrate. The crystalline quality of Ag and In films prepared on PTCDA substrates are found to be superior to films prepared on DiMe-PTCDI films, resulting in work functions being higher by about 200 meV.

Neither metals form abrupt interfaces with the organic films. The interaction between In and the organic substrates is significantly larger than for Ag. A small amount of Ag seems to diffuse via the grain boundaries in the organic film, while substantial diffusion even into the organic crystallites is observed for In. All metal films investigated show so called "gap states" which are attributed to a dynamical charge transfer. Charging of the molecule will result in a geometrical relaxation and a change in the energy position of the HOMO and the LUMO, that is, both will shift into the gap [38]. A polaron state exists with the upper level being half filled and crossed by the Fermi-level, while the lower level is fully occupied. A bipolaron state exists for both levels being fully occupied. For In and Ag deposited on PTCDA and DiMe-PTCDI the gap states induced by the metals are found well below the Fermi-level and are therefore attributed to bipolaron states.

## Acknowledgements

We are grateful to the Bundesministerium fur Bildung und Forschung (BMBF, No. 05 SE8OCA 7) and the EU funded Human Potential Research Training Network "DIODE" (Contract No.: HPRN-CT-1999–00164) for financial support. One of the authors (A.D.) acknowledges funding of his PostDoc stipendium by the Alexander von Humboldt-Stiftung. We also would like to thank Freiberger Compound Materials for their support.

## References

[1] Y. Hirose, A. Kahn, V. Aristov, P. Soukiassian, V. Bulovic, S.R. Forrest, Phys. Rev. B 54 (1996) 13748.

[2] Y. Hirose, A. Kahn, V. Aristov, P. Soukiassian, Appl. Phys. Lett. 68 (1996) 217.

[3] Y. Hirose, C.I. Wu, V. Aristov, P. Soukiassian, A. Kahn, Appl. Surf. Sci. 113/114 (1997) 291.

[4] H. Ishii, K. Sugiyama, E. Ito, K. Seki, Adv. Mater. 11 (1999) 605.

[5] I.G. Hill, A. Rajagopal, A. Kahn, Y. Hu, Appl. Phys. Lett. 73 (1998) 662.

[6] D. Yoshimura, H. Ishii, S. Narioka, M. Sei, T. Miyazaki, Y. Ouchi, S. Hasegawa, Y. Harima, K. Yamashita, K. Seki, J. Electron Relat. Phenom. 78 (1996) 359.

[7] H. Ishii, K. Seki, IEEE Trans. Electron. Dev. 44 (1997) 1295.

[8] I.G. Hill, A. Kahin, in: Proceedings of the SPIE International Symposium on Organic Light Emitting Materials and Devices II 3476 (1998) p. 168.

[9] A. Rajagopal, I.G. Hill, A. Kahn, Cryst. Mol. Cryst. Liq. Sect. A 322 (1998) 245.

[10] H. Ishii, K. Sugiyama, K. Seki, in: Proceedings of the SPIE International Symposium on Organic Light Emitting Materials and Devices (1997) p. 228.

[11] I.G. Hill, A. Rajagopal, A. Kahn, J. Appl. Phys. Lett. 84 (1998) 3236.

[12] H. Peisert, M. Knupfer, J. Fink, Appl. Phys. Lett. 81 (2002) 2400.

[13] I.G. Hill, A. Kahn, Z.G. Soos, A. Pascal Jr., Chem. Phys. Lett. 327 (2001) 181.

[14] I.G. Hill, A.J. Makinen, Z.H. Kafa, Appl. Phys. Lett. 77 (2000) 1825.

[15] N. Ueno, K. Sugita, O. Koga, S. Suzuki, Jpn. J. Appl. Phys. 22 (1983) 1613.

[16] A. Rajagopal, A. Kahn, J. Appl. Phys. Phys. 84 (1998) 355.

[17] N. Johansson, T. Osada, S. Strafström, W.R. Salanek, V. Parente, D.A. dos Santos, X. Crispin, L.J. Bredas, J. Chem. Phys. 11 (1999) 2157.

[18] V.-E. Choong, M.G. Mason, C.W. Tang, Y. Gao, Appl. Phys. Lett. 72 (1998) 2689.

[19] I.G. Hill, J. Schwartz, A. Kahn, Org. Electron. 1 (2000) 5.

[20] M. Pope, C.E. Swenberg, Electronic Processes in Organic Crystals and Polymers, Oxford Science Publication (1999).

[21] Y. Hirose, A. Kahn, V. Aristov, P. Soukiassian, V. Batovic, S.R. Forrest, Phys. Rev. B 54 (1996) 13748.

[22] Y. Azuma, S. Akatsuka, K.K. Okudaira, Y. Harada, N. Ueno, J. Appl. Phys. 87 (2) (2000) 766.

[23] T. Ertl, H.G. Mack, C. Ziegler, Private communication.

[24] T.U. Kampen, G. Salvan, A. Paraian, C. Himcinschi, A.Y. Kobitski, M. Friedrich, D.R.T. Zahn, Appl. Surf. Sci. 212/213 (2003) 501–507.

[25] Y. Hirose, W. Chen, E.I. Haskal, S. R Forrest, A. Kahn, Appl. Phys. Lett. 64 (25) (1994) 3482.

[26] Y. Hirose, S.R. Forrest, A. Kahn, Phys. Rev. B 52 (1995) 14040.

[27] Z.S. Li, W.Z. Cai, R.Z. Su, G.S. Dong, D.M. Huang, X.M. Ding, X.Y. Hou, X. Wang, Appl. Phys. Lett. 64 (25) (1994) 3425.

[28] M.D. Pashley, D. Li, J. Vac. Sci. Technol. A12 (1994) 1848.

[29] Y. Hirose, W. Chen, E.I. Haskal, S.R. Forrest, A. Kahn, J. Vac. Sci. Technol B12 (1994) 2616.

[30] E. Umbaeh, R. Fink, in: V.M. Agranovich, G.C. La Rocca (Eds.), Organic Nanocrystals: Science and Applications, Proceedings of the International School of Physics "Enrico Fermi", Course CXLIX, IOS Press, Netherlands (2002), p. 233.

[31] G. Salvan, PhD Thesis, Chemnitz University of Technology, 2003.

[32] A.W. Dweydari, C.H.B. Mee, Phys. Status Solidi A 17 (1973) 247.

[33] A.W. Dweydari, C.H.B. Mee, Phys. Status Solidi A 27 (1975) 223.

[34] Y. Hirose, A. Kahn, V. Aristov, P. Soukiassian, V. Bulovic, S.R. Forrest, Phys. Rev. B 54 (19) (1996) 13748.

[35] I.G. Hill, A. Rajagopal, A. Kahn, Y. Hu, Appl. Phys. Lett. 73 (5) (1998) 662.

[36] B. Paez, G. Salvan, S. Dilaghi, T.U. Kampen, D.R.T. Zahn, Appl. Surf. Sci. 234 (2004) 168.

[37] S. Kera, H. Setoyama, M. Onoue, K.K. Okudaira, Y. Harada, N. Ueno, Phys. Rev. B 63 (2001) 15204.

[38] D. Steinmüller, M.G. Ramsey, F.P. Netzer, Phys. Rev. B 47 (1993) 13323.